

LINEAR STABILITY THEORY

Serkan Özgen, Prof. Dr.

Middle East Technical University, Dept. Aerospace Eng., Turkey

1. Introduction

Hydrodynamic stability is known as one of the most important and yet least understood fields of fluid mechanics since more than a century. Its main concern is to investigate the **breakdown of laminar flows**, their subsequent development and eventual transition to turbulent flow. A few of the practical applications of this subject are: laminar flow control of wings of large transport aircraft in order to save in fuel consumption, prediction of transition location on airfoils for accurate heat transfer prediction and blade cooling in turbomachinery, and jet flows for more efficient combustion in gas turbine and internal combustion engines, etc.

A summary of the **process of transition** in the boundary-layer over a flat plate is illustrated in Figure 1 [1]. As can be seen from the figure, the flow goes through the following stages, starting with the leading edge [2]:

- i. Stable flow following the leading edge.
- ii. Unstable, laminar flow with two-dimensional Tollmien-Schlichting waves.
- iii. Development of unstable, laminar, three-dimensional unstable waves and vortex formation (hairpin eddies).
- iv. Bursts of turbulence in places of very high vorticity.
- v. Formation of turbulent spots at locally intense fluctuations.
- vi. Coalescence of turbulent spots into a fully developed turbulent boundary-layer.

Evolution of small, **regular oscillations** travelling in laminar boundary-layers was first pointed out by Rayleigh [3] and Prandtl [4]. Tollmien [5] outlined a complete theory of boundary-layer stability and Schlichting [6] calculated the amplification of most unstable frequencies. This is mainly the reason why the instability waves observed in boundary-layer flow are called “Tollmien-Schlichting” waves. However, due to lack of experimental evidence, the Linear Stability theory received very little recognition then. The well-known experiments of Schubauer and Skramstad [7] completely revised this opinion by demonstrating that the Tollmien-Schlichting waves constitute the first stage of the transition process. Formation of Tollmien-Schlichting waves in a flow over a flat plate can be seen in Figure 2 [8].

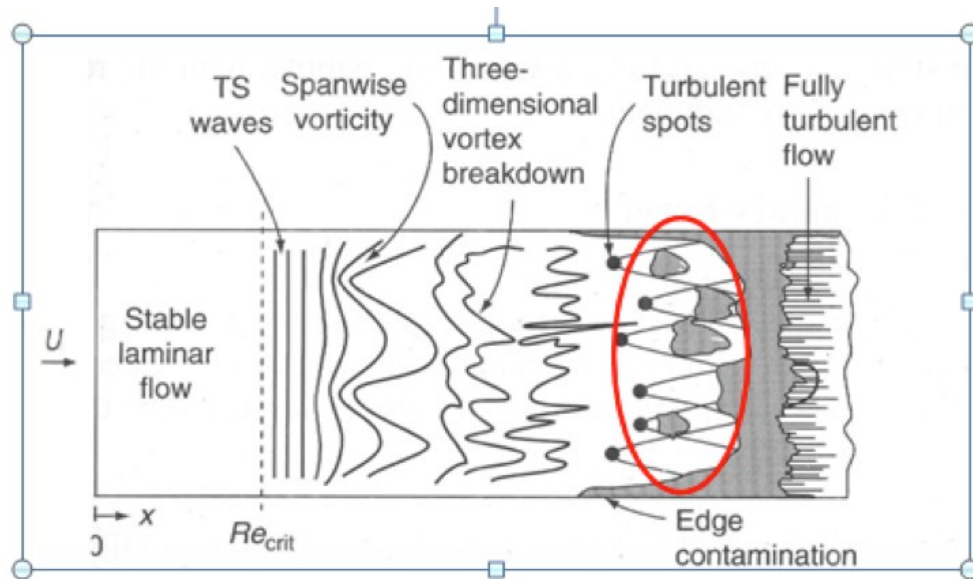


Figure 1. Stages of laminar-turbulent transition on a flat-plate boundary-layer [1].

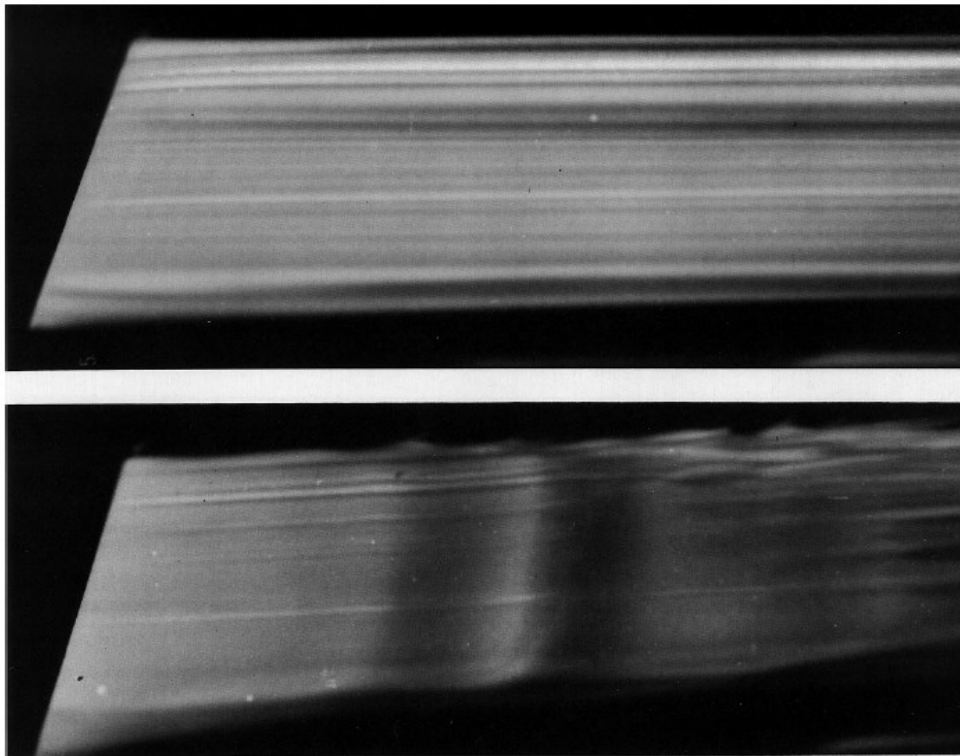


Figure 2. Instability of the boundary-layer over a flat plate aligned with the stream. At $Re=20000$ (upper photo), the flow is laminar. At $Re=100000$ (lower photo), two-dimensional Tollmien-Schlichting waves appear [8].

Linear stability theory, which the current manuscript is based on, deals with the first stage of the transition process, namely the stage starting from the appearance of **sinusoidal disturbances** in the otherwise undisturbed laminar flow until nonlinear interactions between amplified disturbances start occurring. As such, it remains as the most well understood and established part of the entire hydrodynamic stability theory.

In this manuscript, the Linear Stability Theory is outlined resulting in the stability equations. The theory is described for a three-dimensional, steady, incompressible mean flow but it is also applicable to other regimes, see Reference [9]. Well-known and established methods are introduced to clearly illustrate the basics of the theory and to make it easier for the reader to follow the literature. Method of small disturbances, method of normal modes, temporal and spatial formulations, Gaster's Transformation, Orr-Sommerfeld equation and Squire's Theorem are explained. Solution of the eigenvalue problem is also outlined together with the application of the theory to two- and three-dimensional boundary-layer flows.

2. Formulation of the Linear Stability Theory

2.1. Basic Flow

In order to perform the stability analysis of a flow, velocity $\vec{U}^*(\vec{x}^*, t^*)$, pressure $P^*(\vec{x}^*, t^*)$ and temperature $T^*(\vec{x}^*, t^*)$ fields must be known. These fields define the **basic flow**. The basic flow may be steady or unsteady, two-dimensional or three-dimensional, incompressible or compressible and even Newtonian or non-Newtonian, but in any case must satisfy the corresponding equations of motion.

2.2. Method of Small Disturbances

We shall make use of the **method of small disturbances**, which leads to a linear problem. Equations of motion for a three-dimensional, incompressible flow in Cartesian coordinates are (asterisks denote dimensional quantities, while g^* denotes gravitational acceleration):

$$\frac{\partial u^*}{\partial t^*} + u^* \frac{\partial u^*}{\partial x^*} + v^* \frac{\partial u^*}{\partial y^*} + w^* \frac{\partial u^*}{\partial z^*} = -\frac{1}{\rho^*} \frac{\partial p^*}{\partial x^*} + \frac{1}{\rho^*} \left(\frac{\partial \sigma_{xx}^*}{\partial x^*} + \frac{\partial \tau_{xy}^*}{\partial y^*} + \frac{\partial \tau_{xz}^*}{\partial z^*} \right), \quad (1)$$

$$\frac{\partial v^*}{\partial t^*} + u^* \frac{\partial v^*}{\partial x^*} + v^* \frac{\partial v^*}{\partial y^*} + w^* \frac{\partial v^*}{\partial z^*} = -\frac{1}{\rho^*} \frac{\partial p^*}{\partial y^*} + \frac{1}{\rho^*} \left(\frac{\partial \tau_{yx}^*}{\partial x^*} + \frac{\partial \sigma_{yy}^*}{\partial y^*} + \frac{\partial \tau_{yz}^*}{\partial z^*} \right) - g^*, \quad (2)$$

$$\frac{\partial w^*}{\partial t^*} + u^* \frac{\partial w^*}{\partial x^*} + v^* \frac{\partial w^*}{\partial y^*} + w^* \frac{\partial w^*}{\partial z^*} = -\frac{1}{\rho^*} \frac{\partial p^*}{\partial z^*} + \frac{1}{\rho^*} \left(\frac{\partial \tau_{zx}^*}{\partial x^*} + \frac{\partial \tau_{zy}^*}{\partial y^*} + \frac{\partial \sigma_{zz}^*}{\partial z^*} \right), \quad (3)$$

$$\frac{\partial u^*}{\partial x^*} + \frac{\partial v^*}{\partial y^*} + \frac{\partial w^*}{\partial z^*} = 0. \quad (4)$$

In the above equations, ρ^* denotes the density of the fluid. The stress terms are defined as:

$$\sigma_{xx}^* = 2\mu^* \frac{\partial u^*}{\partial x^*}, \quad \sigma_{yy}^* = 2\mu^* \frac{\partial v^*}{\partial y^*}, \quad \sigma_{zz}^* = 2\mu^* \frac{\partial w^*}{\partial z^*}, \quad (5)$$

$$\tau_{xy}^* = \tau_{yx}^* = \mu^* \left(\frac{\partial u^*}{\partial y^*} + \frac{\partial v^*}{\partial x^*} \right), \quad (6)$$

$$\tau_{xz}^* = \tau_{zx}^* = \mu^* \left(\frac{\partial u^*}{\partial z^*} + \frac{\partial w^*}{\partial x^*} \right), \quad (7)$$

$$\tau_{yz}^* = \tau_{zy}^* = \mu^* \left(\frac{\partial v^*}{\partial z^*} + \frac{\partial w^*}{\partial y^*} \right). \quad (8)$$

In the above equations, μ^* is the viscosity of the fluid.

The flow is decomposed into steady mean and unsteady perturbations as follows:

$$u^*(x^*, y^*, z^*, t^*) = U^*(x^*, y^*, z^*) + \hat{u}^*(x^*, y^*, z^*, t^*), \quad (9)$$

$$v^*(x^*, y^*, z^*, t^*) = V^*(x^*, y^*, z^*) + \hat{v}^*(x^*, y^*, z^*, t^*), \quad (10)$$

$$w^*(x^*, y^*, z^*, t^*) = W^*(x^*, y^*, z^*) + \hat{w}^*(x^*, y^*, z^*, t^*), \quad (11)$$

$$p^*(x^*, y^*, z^*, t^*) = P^*(x^*, y^*, z^*) + \hat{p}^*(x^*, y^*, z^*, t^*). \quad (12)$$

The problem is further simplified when the **parallel flow assumption** is employed. Accordingly, $U^* = U^*(y^*)$, $W^* = W^*(y^*)$ only, and $V^* = 0$. In a channel flow, such a flow is reproduced with great accuracy at a large distance from the inlet. Boundary-layer flow can also be regarded as a good approximation because $U^* \gg V^*$ and $\partial/\partial y^* \gg \partial/\partial x^*$. For pressure, it is necessary to retain dependence both on x^* and y^* , because pressure gradient $\partial p^*/\partial x^*$ drives the flow in most cases. Therefore, equations (7-9) can be rewritten as:

$$u^*(x^*, y^*, z^*, t^*) = U^*(y^*) + \hat{u}^*(x^*, y^*, z^*, t^*), \quad (13)$$

$$v^*(x^*, y^*, z^*, t^*) = \hat{v}^*(x^*, y^*, z^*, t^*), \quad (14)$$

$$w^*(x^*, y^*, z^*, t^*) = W^*(y^*) + \hat{w}^*(x^*, y^*, z^*, t^*), \quad (15)$$

$$p^*(x^*, y^*, z^*, t^*) = P^*(x^*, y^*, z^*) + \hat{p}^*(x^*, y^*, z^*, t^*). \quad (16)$$

In the next step, the flow defined in equations (13-16) is substituted into equations (1-4). Unsteady perturbations are small with respect to their counterparts, i.e. $\hat{u}^*, \hat{v}^* \ll U^*$, therefore quadratic terms like $\hat{u}^* \partial \hat{u}^*/\partial x^*$ are dropped out and the following set of equations result:

$$\frac{\partial \hat{u}^*}{\partial t^*} + U^* \frac{\partial \hat{u}^*}{\partial x^*} + \hat{v}^* \frac{dU^*}{dy^*} + W^* \frac{\partial \hat{u}^*}{\partial z^*} = -\frac{1}{\rho^*} \left(\frac{\partial P^*}{\partial x^*} + \frac{\partial \hat{p}^*}{\partial x^*} \right) + \nu^* \left(\frac{d^2 U^*}{dy^{*2}} + \frac{\partial^2 \hat{u}^*}{\partial x^{*2}} + \frac{\partial^2 \hat{u}^*}{\partial y^{*2}} + \frac{\partial^2 \hat{u}^*}{\partial z^{*2}} \right), \quad (17)$$

$$\frac{\partial \hat{v}^*}{\partial t^*} + U^* \frac{\partial \hat{v}^*}{\partial x^*} + W^* \frac{\partial \hat{v}^*}{\partial z^*} = -\frac{1}{\rho^*} \left(\frac{\partial P^*}{\partial y^*} + \frac{\partial \hat{p}^*}{\partial y^*} \right) + \nu^* \left(\frac{\partial^2 \hat{v}^*}{\partial x^{*2}} + \frac{\partial^2 \hat{v}^*}{\partial y^{*2}} + \frac{\partial^2 \hat{v}^*}{\partial z^{*2}} \right) - g^*, \quad (18)$$

$$\frac{\partial \hat{w}^*}{\partial t^*} + U^* \frac{\partial \hat{w}^*}{\partial x^*} + \hat{v}^* \frac{dW^*}{dy^*} + W^* \frac{\partial \hat{w}^*}{\partial z^*} = -\frac{1}{\rho^*} \left(\frac{\partial P^*}{\partial z^*} + \frac{\partial \hat{p}^*}{\partial z^*} \right) + \nu^* \left(\frac{d^2 W^*}{dy^{*2}} + \frac{\partial^2 \hat{w}^*}{\partial x^{*2}} + \frac{\partial^2 \hat{w}^*}{\partial y^{*2}} + \frac{\partial^2 \hat{w}^*}{\partial z^{*2}} \right) \quad (19)$$

$$\frac{\partial \hat{u}^*}{\partial x^*} + \frac{\partial \hat{v}^*}{\partial y^*} + \frac{\partial \hat{w}^*}{\partial z^*} = 0. \quad (20)$$

In the above equations, $\nu^* = \mu^*/\rho^*$ is the kinematic viscosity of the fluid. It is worth mentioning that the perturbation velocities satisfy the continuity equation.

At this point, non-dimensionalization of velocities with an appropriate velocity scale U_{ref}^* , and lengths with an appropriate length scale d_{ref}^* is performed. Accordingly, time is normalized by d_{ref}^*/U_{ref}^* and pressure by $\rho^* U_{ref}^{*2}$.

After the terms involving only the basic flow quantities are dropped, the following set of equations is obtained:

$$\frac{\partial \hat{u}}{\partial t} + U \frac{\partial \hat{u}}{\partial x} + W \frac{\partial \hat{u}}{\partial z} + \hat{v} \frac{dU}{dy} = -\frac{\partial \hat{p}}{\partial x} + \frac{1}{Re} \left(\frac{\partial^2 \hat{u}}{\partial x^2} + \frac{\partial^2 \hat{u}}{\partial y^2} + \frac{\partial^2 \hat{u}}{\partial z^2} \right), \quad (21)$$

$$\frac{\partial \hat{v}}{\partial t} + U \frac{\partial \hat{v}}{\partial x} + W \frac{\partial \hat{v}}{\partial z} = -\frac{\partial \hat{p}}{\partial y} + \frac{1}{Re} \left(\frac{\partial^2 \hat{v}}{\partial x^2} + \frac{\partial^2 \hat{v}}{\partial y^2} + \frac{\partial^2 \hat{v}}{\partial z^2} \right), \quad (22)$$

$$\frac{\partial \hat{w}}{\partial t} + U \frac{\partial \hat{w}}{\partial x} + W \frac{\partial \hat{w}}{\partial z} + \hat{v} \frac{dW}{dy} = -\frac{\partial \hat{p}}{\partial z} + \frac{1}{Re} \left(\frac{\partial^2 \hat{w}}{\partial x^2} + \frac{\partial^2 \hat{w}}{\partial y^2} + \frac{\partial^2 \hat{w}}{\partial z^2} \right), \quad (23)$$

$$\frac{\partial \hat{u}}{\partial x} + \frac{\partial \hat{v}}{\partial y} + \frac{\partial \hat{w}}{\partial z} = 0. \quad (24)$$

In the above equations, Reynolds number is defined as $Re = U_{ref}^* d_{ref}^* / \nu^*$. In equation (18):

$$-\frac{1}{\rho^*} \frac{\partial P^*}{\partial y^*} - g^* = 0 \quad \text{or} \quad \frac{\partial P}{\partial y} + Fr^{-2} = 0, \quad (25)$$

where $Fr = U_{ref}^* / (g^* d_{ref}^*)^{1/2}$ is the Froude number.

2.3. Method of Normal Modes

The basic laminar flow in x-direction is assumed to be influenced by a disturbance composed of a number of discrete partial fluctuations each consisting of a wave propagating in x-direction. Perturbation velocities corresponding to each component can be defined as:

$$[\hat{u}, \hat{v}, \hat{w}, \hat{p}] = [\bar{u}, \bar{v}, \bar{w}, \bar{p}](y) e^{i(\alpha x + \beta z - \omega t)}, \quad j = 1, 2, 3, \dots \quad (26)$$

In the above equation, $\bar{u}(y)$, $\bar{v}(y)$, $\bar{w}(y)$ and $\bar{p}(y)$ are the **disturbance amplitude functions** for the perturbations \hat{u} , \hat{v} , \hat{w} and \hat{p} . The disturbance **wavenumber components** are α and β . The **frequency of the disturbance** is denoted by ω . In the general formulation, wavenumber components α and β , and the frequency ω are complex.

Normal mode decomposition is a Fourier analysis of the disturbance modes based on the fact that all the coefficients in equations (21-24) are functions of y only, admitting Fourier modes in x, z and t .

When the definitions in equation (26) are substituted into equations (21-24), the following system of equations result (primes (') denoting differentiation with respect to y):

$$i(\alpha U + \beta W - \omega)\bar{u} + U' \bar{v} = -i\alpha \bar{p} + \frac{1}{Re} [\bar{u}'' - (\alpha^2 + \beta^2)\bar{u}], \quad (27)$$

$$i(\alpha U + \beta W - \omega)\bar{v} = -\bar{p}' + \frac{1}{Re} [\bar{v}'' - (\alpha^2 + \beta^2)\bar{v}], \quad (28)$$

$$i(\alpha U + \beta W - \omega)\bar{w} + W' \bar{v} = -i\beta \bar{p} + \frac{1}{Re} [\bar{w}'' - (\alpha^2 + \beta^2)\bar{w}], \quad (29)$$

$$i(\alpha \bar{u} + \beta \bar{w}) + \bar{v}' = 0. \quad (30)$$

Equations (27-30) are the perturbation equations for a three-dimensional basic flow in a three-dimensional disturbance environment. They constitute a sixth order system for the variables $\bar{u}, \bar{v}, \bar{w}, \bar{p}, \bar{u}'$ and \bar{w}' . The boundary conditions are:

$$\bar{u}(0) = \bar{v}(0) = \bar{w}(0) = 0, \quad (\text{no slip}) \quad (31)$$

$$\bar{u}(y) \rightarrow 0, \bar{v}(y) \rightarrow 0, \bar{w}(y) \rightarrow 0 \quad \text{as } y \rightarrow \infty. \quad (\text{freestream}) \quad (32)$$

2.4. Temporal and Spatial Amplification Formulations

2.4.1. Spatial Amplification Formulation

In this formulation, the local mode is given as in equation (26). The wave number components are complex, i.e. $\alpha = \alpha_r + i\alpha_i$ and $\beta = \beta_r + i\beta_i$, while the frequency ω is real.

A real **wavenumber vector** can be defined with magnitude:

$$k = (\alpha_r^2 + \beta_r^2)^{1/2}, \quad (33)$$

and a wave angle:

$$\Psi = \tan^{-1}(\beta_r/\alpha_r). \quad (34)$$

The **phase speed** of the wave is defined as $c = \omega/k$.

Accordingly, in spatial amplification formulation, equation (26) can be written as follows:

$$[\hat{u}, \hat{v}, \hat{w}, \hat{p}] = [\bar{u}, \bar{v}, \bar{w}, \bar{p}](y)e^{-\alpha_i x} e^{i(\alpha_r x + \beta z - \omega t)}. \quad (35)$$

The **spatial amplification rate** is $-\alpha_i$ for which:

$\alpha_i < 0$; unstable wave,

$\alpha_i = 0$; neutrally stable wave,

$\alpha_i > 0$; stable wave.

The dispersion relation is given as $\alpha = f(\omega, \beta, Re)$.

2.4.2. Temporal Amplification Formulation

In this formulation, the local mode is still given as in equation (26) but this time the wavenumbers α and β are real and the frequency is complex, $\omega = \omega_r + i\omega_i$. Therefore, phase velocity is also complex, $c = \omega/\alpha = c_r + ic_i$. The **phase speed** of the wave is c_r , and c_i is the **temporal amplification factor**.

Real wavenumber vector magnitude is given as:

$$k = (\alpha^2 + \beta^2)^{1/2}, \quad (36)$$

while the wave angle is:

$$\Psi = \tan^{-1}(\beta/\alpha). \quad (37)$$

Accordingly, equation (26) can be written as follows:

$$[\hat{u}, \hat{v}, \hat{w}, \hat{p}] = [\bar{u}, \bar{v}, \bar{w}, \bar{p}](y)e^{\alpha c_i t} e^{i(\alpha x + \beta z - \alpha c_r t)}. \quad (38)$$

The **temporal amplification rate** is $\omega_i = \alpha c_i$ for which:

- $c_i > 0$; unstable wave,
- $c_i = 0$; neutrally stable wave,
- $c_i < 0$; stable wave.

The dispersion relation is given as $c = f(\alpha, \beta, Re)$.

Since the eigenvalue c appears linearly in the temporal form of the differential equations, most of the early studies reported in the literature are concentrated on this formulation. However, spatial modes seem to describe the observed instability of parallel flows more faithfully than temporal modes.

2.4.3. Gaster's Transformation

It has been shown that simple relations exist between the parameters arising in temporal and spatial amplification formulations [10]. These relations do not constitute a transformation of a time-dependent solution into a spatially dependent one but merely provide a link between the values of the parameters existing in the two problems. Accordingly, the real parts of the wavenumbers and phase velocities are equal in both cases; $\alpha(T) = \alpha_r(S)$, $\beta(T) = \beta_r(T)$ and $c_r(T) = c(S)$. It follows that:

$$\frac{\omega_i(T)}{\alpha_i(S)} = -\frac{\partial \omega_r}{\partial \alpha}. \quad (41)$$

The quantity on the right side of the equation is the **group velocity** and the relation given in this equation is the **Gaster's transformation**. It merely means that the spatial growth of a mode is related to the temporal growth by the group velocity but not the phase velocity.

2.5. Reduction to Fourth Order System

A new set of equations can be obtained by producing linear combinations of equations (27) and (29). Equations (27) and (29) are multiplied by α and β , respectively, and added; equation (27) multiplied by β is subtracted from equation (29) multiplied by α :

$$i(\alpha U + \beta W - \omega)(\alpha \bar{u} + \beta \bar{w}) + (\alpha U' + \beta W')\bar{v} = -i(\alpha^2 + \beta^2)\bar{p} + \frac{1}{Re}[D^2 - (\alpha^2 + \beta^2)](\alpha \bar{u} + \beta \bar{w}), \quad (42)$$

$$i(\alpha U + \beta W - \omega)\bar{v} = -\bar{p}' + \frac{1}{Re}[\bar{v}'' - (\alpha^2 + \beta^2)\bar{v}], \quad (43)$$

$$i(\alpha U + \beta W - \omega)(\alpha \bar{w} - \beta \bar{u}) + (\alpha W' - \beta U')\bar{v} = +\frac{1}{Re}[D^2 - (\alpha^2 + \beta^2)](\alpha \bar{w} - \beta \bar{u}), \quad (44)$$

$$i(\alpha \bar{u} + \beta \bar{w}) + \bar{v}' = 0. \quad (45)$$

In this formulation, the dependent variables are $\alpha\bar{u} + \beta\bar{w}$, \bar{v} , \bar{p} and $\alpha\bar{u}' + \beta\bar{w}'$. Noticing that the variable $\alpha\bar{w} - \beta\bar{u}$ appears only in equation (44), the remaining equations constitute a fourth order system for the solution of the eigenvalues α , β , ω and Re . In physical terms, equation (42) is the momentum equation in the direction of the wave motion, while equation (44) is the momentum equation in the direction perpendicular to wave motion.

2.6. Orr-Sommerfeld Equation

In equation (42), when the $(\alpha\bar{u} + \beta\bar{w})$ term is eliminated by using equation (45) and the pressure term is eliminated by using equation (43), a single fourth order equation results:

$$\bar{v}'''' - 2(\alpha^2 + \beta^2)\bar{v}'' + (\alpha^2 + \beta^2)^2\bar{v} = iRe\{(\alpha U + \beta W - \omega)[\bar{v}'' - (\alpha^2 + \beta^2)\bar{v}] - (\alpha U'' + \beta W'')\bar{v}\}. \quad (46)$$

This is the well-known **Orr-Sommerfeld equation**, which has been the basis for many studies related to incompressible flow study. The accompanying boundary conditions are:

$$\bar{v}(0) = \bar{v}'(0) = 0, \quad (\text{no slip}) \quad (47)$$

$$\bar{v}(y) \rightarrow 0, \quad \bar{v}'(y) \rightarrow 0 \quad \text{as } y \rightarrow \infty. \quad (\text{freestream}) \quad (48)$$

The same equation can be derived in terms of a disturbance streamfunction for a two-dimensional basic flow and a two-dimensional disturbance environment, as detailed in References [2, 11] and many others:

$$\phi'''' - 2\alpha^2\phi'' + \alpha^4\phi = iRe\{(\alpha U - \omega)[\phi'' - \alpha^2\phi] - \alpha U''\phi\}, \quad (49)$$

$$\text{or } \bar{v}'''' - 2\alpha^2\bar{v}'' + \alpha^4\bar{v} = iRe\{(\alpha U - \omega)[\bar{v}'' - \alpha^2\bar{v}] - \alpha U''\bar{v}\}. \quad (50)$$

2.7. Squire's Transformation and Squire's Theorem

For a two-dimensional basic flow ($W = 0$), the following transformation is considered:

$$\begin{aligned} \tilde{\alpha}^2 &= \alpha^2 + \beta^2, & \tilde{\alpha}\tilde{u} &= \alpha\bar{u} + \beta\bar{w}, & \frac{\tilde{p}}{\tilde{\alpha}} &= \frac{\bar{p}}{\alpha}, & \tilde{c} &= c, \\ \tilde{v} &= v, & \tilde{\alpha}\tilde{Re} &= \alpha Re, & \tilde{\omega}\tilde{Re} &= \omega Re. \end{aligned} \quad (51)$$

With this, equations (27-30) become:

$$i(\tilde{\alpha}U - \tilde{\omega})\tilde{u} + U'\tilde{v} = -i\tilde{\alpha}\tilde{p} + \frac{1}{\tilde{Re}}(\tilde{u}'' - \tilde{\alpha}^2\tilde{u}), \quad (52)$$

$$i(\tilde{\alpha}U - \tilde{\omega})\tilde{v} = -\tilde{p}' + \frac{1}{\tilde{Re}}(\tilde{v}'' - \tilde{\alpha}^2\tilde{v}), \quad (53)$$

$$i\tilde{\alpha}\tilde{u} + \tilde{v}' = 0. \quad (54)$$

The three-dimensional problem defined by equations (27-30) has been reduced to an equivalent two-dimensional problem. This transformation relates the eigenvalues of an oblique temporal wave with frequency ω , at Reynolds number Re , to a two-dimensional wave with frequency $\tilde{\omega}$ in a two-dimensional boundary-layer at Reynolds number \tilde{Re} .

Since $\tilde{\alpha}^2 = \alpha^2 + \beta^2 \geq \alpha^2$, it follows that $\widetilde{Re} \leq Re$. Therefore, according to **Squire's Theorem**, two-dimensional disturbances yield the lowest limit of stability. In other words, in order to obtain the minimum critical Reynolds number, it is sufficient to consider two-dimensional disturbances only.

3. Solution Method [12]

In the solution method that is outlined below, temporal amplification formulation is used due to its simpler and more straightforward solution. This does not reduce its validity or accuracy and the method that is outlined can be extended to handle compressible flows, flows with variable fluid properties, etc. [13, 14, 15].

3.1. System of First Order Equations

Defining the following variables:

$$Y_1 = \alpha\bar{u} + \beta\bar{w}, \quad (55)$$

$$Y_2 = \alpha\bar{u}' + \beta\bar{w}', \quad (56)$$

$$Y_3 = \bar{v}, \quad (57)$$

$$Y_4 = \bar{p}, \quad (58)$$

$$Y_5 = \alpha\bar{w} - \beta\bar{u}, \quad (59)$$

$$Y_6 = \alpha\bar{w}' - \beta\bar{u}', \quad (60)$$

equations (42-45) can be written as:

$$Y_1' = Y_2, \quad (61)$$

$$Y_2' = [\alpha^2 + \beta^2 + iRe(\alpha U + \beta W - \omega)]Y_1 + Re(\alpha U' + \beta W')Y_3 + iRe(\alpha^2 + \beta^2)Y_4, \quad (62)$$

$$Y_3' = -iY_1, \quad (63)$$

$$Y_4' = -\frac{i}{Re}Y_2 - \left[\frac{\alpha^2 + \beta^2}{Re} + i(\alpha U + \beta W - \omega) \right] Y_3, \quad (64)$$

$$Y_5' = Y_6, \quad (65)$$

$$Y_6' = Re(\alpha W' - \beta U')Y_3 + [\alpha^2 + \beta^2 + iRe(\alpha U + \beta W - \omega)]Y_5. \quad (66)$$

Boundary conditions:

$$Y_1(0) = Y_3(0) = Y_5(0) = 0, \quad (\text{no slip}) \quad (67)$$

$$Y_1(y) \rightarrow 0, \quad Y_3(y) \rightarrow 0, \quad Y_5(y) \rightarrow 0 \quad \text{as } y \rightarrow \infty. \quad (\text{freestream}) \quad (68)$$

Eigenvalues α , β , ω and Re can be computed by solving equations (61-64) only because variables Y_5 and Y_6 appear only in equations (65) and (66). In other words, equations (65) and (66) are decoupled from equations (61-64).

3.2. Characteristic Values, Characteristic Vector, Solution Vector

In the freestream, the basic flow is uniform and equations (61-66) have constant coefficients. Therefore, the equations and the boundary conditions are homogeneous, and the system given in equations (61-66) constitutes an **eigenvalue problem**, where the **eigenvalues** are α , β , ω and Re . The equations and the boundary conditions are satisfied for certain combinations of the eigenvalues for a non-trivial solution. As such, the system of equations allow solutions:

$$\vec{Z}_{(i)} = \vec{A}_{(i)}e^{\lambda_i y}, \quad i = 1,6. \quad (69)$$

In the above, $\vec{Z}_{(i)}$ and $\vec{A}_{(i)}$ are the six component solution and characteristics vectors, respectively, while λ_i are the characteristic values. These are computed by using linear algebra.

3.2.1. Characteristic values

Characteristic values are computed as follows:

$$\lambda_{1,2} = \mp(\alpha^2 + \beta^2)^{1/2}, \quad (70)$$

$$\lambda_{3,4} = \mp[\alpha^2 + \beta^2 + iRe(\alpha U_e + \beta W_e - \omega)]^{1/2}, \quad (71)$$

$$\lambda_{5,6} = \mp[\alpha^2 + \beta^2 + iRe(\alpha U_e + \beta W_e - \omega)]^{1/2}. \quad (72)$$

Here, U_e and W_e are the values of the dimensionless velocity components at the freestream (which are usually 1 and 0, respectively). Because of the freestream boundary conditions given in equation (68), characteristic values with a minus sign are of physical interest.

3.2.2. Characteristic vectors:

Characteristic vector corresponding to $\lambda_1 = -(\alpha^2 + \beta^2)^{1/2}$:

$$\chi_{11} = -i(\alpha^2 + \beta^2)^{1/2}, \quad (73)$$

$$\chi_{12} = i(\alpha^2 + \beta^2), \quad (74)$$

$$\chi_{13} = 1, \quad (75)$$

$$\chi_{14} = i \frac{(\alpha U_e + \beta W_e - \omega)}{(\alpha^2 + \beta^2)^{1/2}}, \quad (76)$$

$$\chi_{15} = 0, \quad (77)$$

$$\chi_{16} = 0. \quad (78)$$

Characteristic vector corresponding to $\lambda_3 = -[\alpha^2 + \beta^2 + iRe(\alpha U_e + \beta W_e - \omega)]^{1/2}$:

$$\chi_{31} = 1, \quad (79)$$

$$\chi_{32} = -[\alpha^2 + \beta^2 + iRe(\alpha U_e + \beta W_e - \omega)]^{1/2}, \quad (80)$$

$$\chi_{33} = \frac{i}{[\alpha^2 + \beta^2 + iRe(\alpha U_e + \beta W_e - \omega)]^{1/2}}, \quad (81)$$

$$\chi_{34} = 0, \quad (82)$$

$$\chi_{35} = 0, \quad (83)$$

$$\chi_{36} = 0. \quad (84)$$

Characteristic vector corresponding to $\lambda_5 = -[\alpha^2 + \beta^2 + iRe(\alpha U_e + \beta W_e - \omega)]^{1/2}$:

$$\chi_{51} = \chi_{52} = \chi_{53} = \chi_{54} = 0, \quad (85)$$

$$\chi_{55} = 1, \quad (86)$$

$$\chi_{56} = -[\alpha^2 + \beta^2 + iRe(\alpha U_e + \beta W_e - \omega)]^{1/2}. \quad (87)$$

The solution corresponding to λ_1 is referred to as the inviscid solution, while solutions corresponding to λ_3 and λ_5 are the first and second viscous solutions, respectively.

3.2.3. Solution Vector:

The general solution vector is a linear combination of the characteristic vectors corresponding to three characteristic values given above:

$$Y_1(y) = -c_1 i(\alpha^2 + \beta^2)^{1/2} e^{\lambda_1 y} + c_3 e^{\lambda_3 y}, \quad (88)$$

$$Y_2(y) = c_1 i(\alpha^2 + \beta^2) e^{\lambda_1 y} - c_3 [\alpha^2 + \beta^2 + iRe(\alpha U_e + \beta W_e - \omega)]^{1/2} e^{\lambda_3 y}, \quad (89)$$

$$Y_3(y) = c_1 e^{\lambda_1 y} + c_3 \frac{i}{[\alpha^2 + \beta^2 + iRe(\alpha U_e + \beta W_e - \omega)]^{1/2}} e^{\lambda_3 y}, \quad (90)$$

$$Y_4(y) = c_1 \frac{i(\alpha U_e + \beta W_e - \omega)}{(\alpha^2 + \beta^2)^{1/2}} e^{\lambda_1 y}, \quad (91)$$

$$Y_5(y) = c_5 e^{\lambda_5 y}, \quad (92)$$

$$Y_6(y) = -c_5 [\alpha^2 + \beta^2 + iRe(\alpha U_e + \beta W_e - \omega)]^{1/2} e^{\lambda_5 y}. \quad (93)$$

In the above equations, c_1 , c_3 and c_5 are arbitrary constants. The solutions given in equations (88-93) provide the initial conditions for the integration of equations (61-66). For integration, a variable stepsize fourth order Runge-Kutta integrator is used. As the integration proceeds from the freestream towards the wall, the viscous solution grows much faster than the inviscid solution due to the presence of the Re term and the linear independence between the two solutions is lost. Therefore, **Gram-Schmidt Orthonormalization** needs to be applied at regular intervals of integration [11, 12]. When the wall is reached, the no slip boundary condition given in equation (67) must be satisfied. This will be possible only for certain combinations of the eigenvalues α , β , ω and Re . In the present solution method, three of these parameters are fixed, and the remaining two are sought (remember that ω is complex and therefore counts as two parameters).

The computation of the correct pair (α, c_r) for fixed (Ψ, Re, c_i) requires a refined search and iteration procedure for a rapid generation of the stability characteristics. To plot the stability curves in the $Re - \alpha$ plane like the ones shown in Figure 3, one needs to start with two known points on the curve so that iteration can proceed in the negative Re direction for the remaining points. The first two points on the curve are calculated using a function minimization routine utilizing the Simplex Method. Once these points are found, the remaining points are computed by a much faster **Newton Iteration Method** in two variables [11].

4. Results

4.1. Two-Dimensional Basic Flow with Pressure Gradient

Looking at equations (61-66), it can be seen that the velocity components U and W must be specified together with their first derivatives, U' and W' . For the solutions to proceed successfully, velocity profiles need to be produced with great accuracy. For two-dimensional flows ($W = 0$) with pressure gradient, the well-known Falkner-Skan equation can be used:

$$2f''' + ff' + \beta_H(1 - f'^2) = 0, \quad (94)$$

where $f' = U$, $\beta_H = 2m/m + 1$; Falkner-Skan or Hartree parameter, and:

$$m = \frac{x^*}{U_e^*} \frac{dU_e^*}{dx^*}; \quad \text{pressure gradient parameter.} \quad (95)$$

The sign of the Hartree parameter determines the pressure gradient:

$\beta_H < 0$; flows with adverse pressure gradient,

$\beta_H = 0$; flow over a flat plate, a.k.a. Blasius flow,

$\beta_H > 0$; flows with favourable pressure gradient.

Non-dimensionalization is done with respect to the Falkner-Skan length scale:

$$d_{ref}^* = \sqrt{\frac{v^* x^*}{(m+1)U_e^*}}. \quad (96)$$

As for the velocity scale, the boundary-layer limiting freestream velocity, U_e^* is used. Equation (94) is subject to the no-slip boundary condition at the wall and the freestream condition:

$$f(0) = f'(0) = 0, \quad (\text{no slip}) \quad (97)$$

$$f'(y) \rightarrow 0 \quad \text{as} \quad y \rightarrow \infty. \quad (\text{freestream}) \quad (98)$$

During the solution process, equation (94) is integrated simultaneously with equations (61-66) starting from the freestream proceeding towards the wall.

Figure 3 shows the constant amplification factor curves for the Blasius flow. The region remaining inside the $c_i=0$ curve is the unstable domain, whereas the remaining region is the stable domain. As can be seen from the figure, below a certain value of the Reynolds number, all waves are stable. However, beyond this value, at least some of the waves are amplified. This is the **critical Reynolds number**, and is one of the most important parameters of the linear stability theory. In this figure, non-dimensionalization is made respect to the boundary-layer displacement thickness, δ_1^* . For Falkner-Skan profiles, this is always a constant multiple of the Falkner-Skan length scale as can be seen in the second column of Table 1, which also depicts the critical Reynolds number values for various Falkner-Skan profiles.

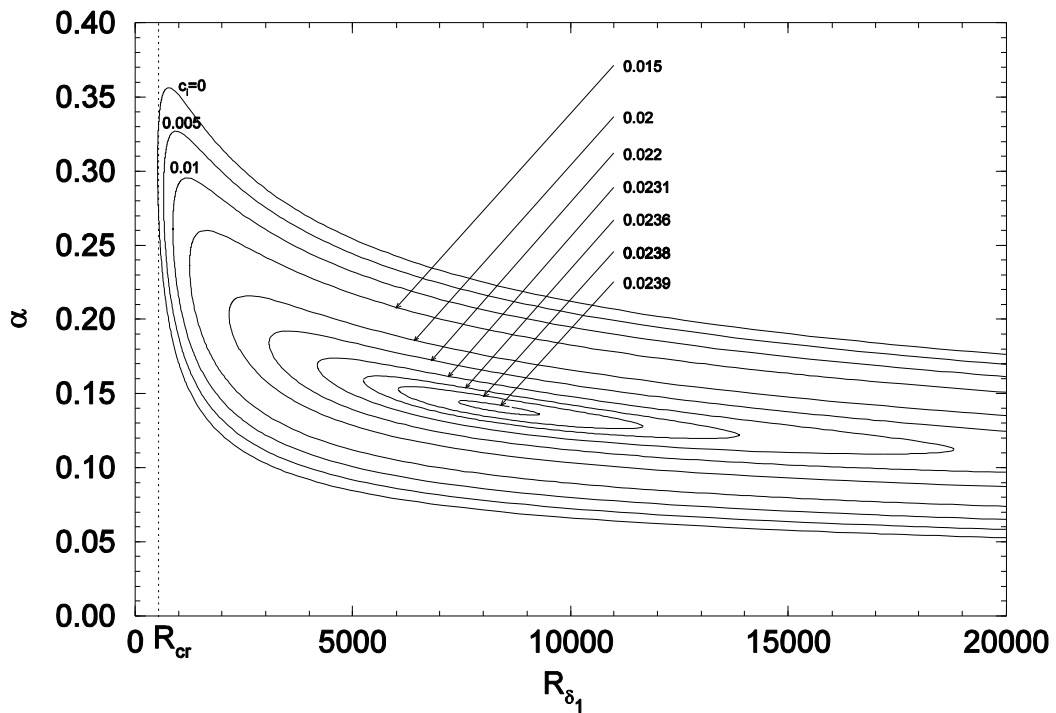


Figure 3. Constant amplification factor curves for $\beta_H = 0$ (Blasius flow) [11].

Table 1. Variation of the critical Reynolds number as a function of β_H [11].

β	δ_1^*/d^*	Re_{cr} (present method)	Re_{cr} (Obremski et al.)
-0.1988	3.29933	67	67
-0.10	2.04028	198	199
-0.05	1.85596	316	318
0.0	1.72079	519	520
0.1	1.52780	1370	1380
0.2	1.39181	2833	2830
0.3	1.29834	4569	4550
0.4	1.20582	6165	6230
0.5	1.13678	7610	7680
0.6	1.08042	8873	8890
0.8	0.98808	10880	10920
1.0	0.91627	12595	12490

Figure 4 illustrates the neutral stability curves ($c_i = 0$) for various Falkner-Skan profiles. It can be seen that for $\beta_H < 0$, the unstable regions are larger and the critical Reynolds numbers are less than for $\beta_H > 0$ as expected.

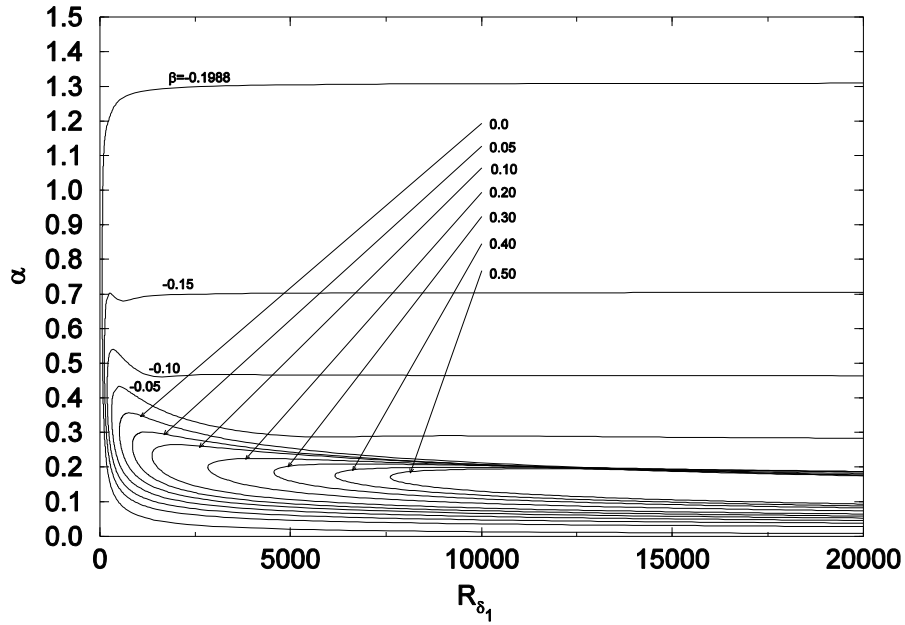


Figure 4. Neutral stability curves for different Falkner-Skan flows [11].

4.2. Three-Dimensional Basic Flow with Pressure Gradient

The stability characteristics of three-dimensional basic flows can be studied systematically using the Falkner-Skan-Cooke profiles. A wedge with a non-zero sweep angle is considered as shown in Figure 5. This way, the flow in the chordwise direction and perpendicular to it can be studied systematically using two parameters. The first of these parameters is the Falkner-Skan or Hartree parameter β_H , while the second one is the angle defining the ratio of the freestream velocity component in the direction of the leading edge to the component in the chord direction, denoted θ .

Flow in the chordwise direction, x_c is defined by the Falkner-Skan equation (repeated):

$$2f''' + ff' + \beta_H(1 - f'^2) = 0. \quad (94)$$

Flow in the spanwise direction, z_s is defined by the following equation:

$$g'' + fg' = 0. \quad (99)$$

The boundary conditions for the solution of equations (94) and (99) are as follows:

$$f'(0) = g(0) = 0, \quad (\text{no slip}) \quad (100)$$

$$f'(y) \rightarrow 1, g(y) \rightarrow 1 \quad \text{as} \quad y \rightarrow \infty. \quad (\text{freestream}) \quad (101)$$

For the profiles obtained from equations (94) and (99) to be used in equations (61-66), they need to be expressed in x and z directions as shown in Figure 5. These components are computed using the flow angle θ as follows:

$$U(y) = f'(y) \cos^2 \theta + g(y) \sin^2 \theta, \quad (102)$$

$$W(y) = [-f'(y) + g(y)] \cos \theta \sin \theta. \quad (103)$$

Examples to profiles thus obtained are presented in Figures 6, 7 and 8 for $\beta_H = -0.05, 0, 0.1$ and $\theta = 45^\circ$ [16]. Figure 9 depicts a composite profile $\beta_H = -0.1$ and $\theta = 45^\circ$ [16].

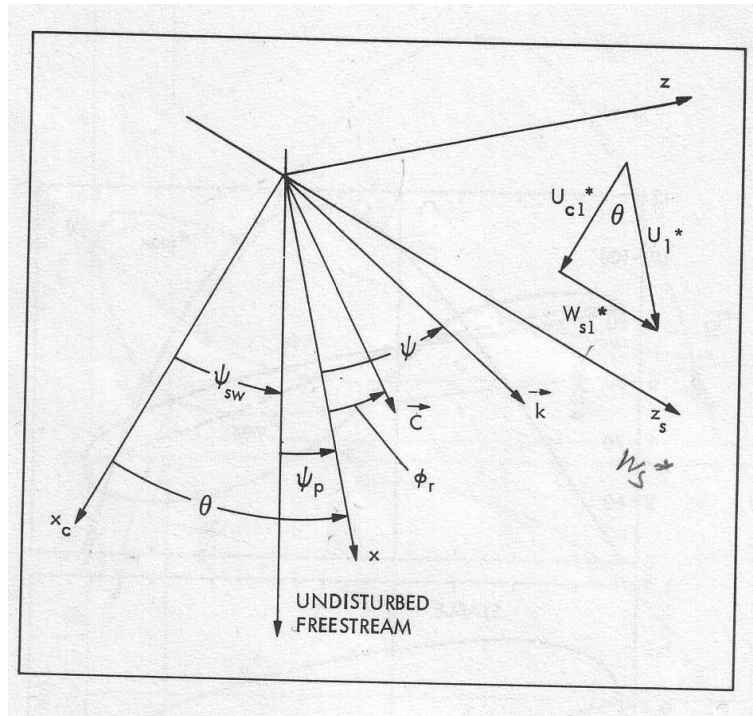


Figure 5. Flow geometry for three-dimensional flow analysis [12].

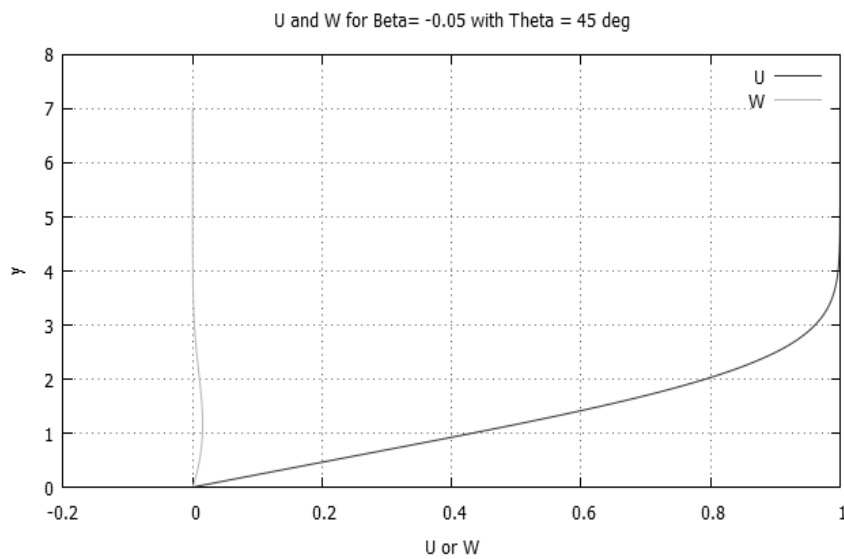


Figure 6. Velocity profiles for $\beta_H = -0.05$ and $\theta = 45^\circ$ [16].

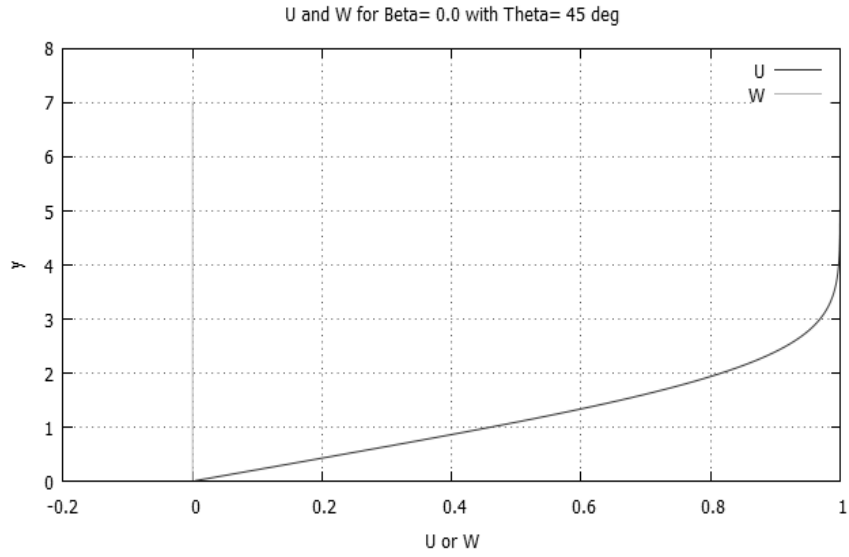


Figure 7. Velocity profiles for $\beta_H = 0$ and $\theta = 45^\circ$ [16].

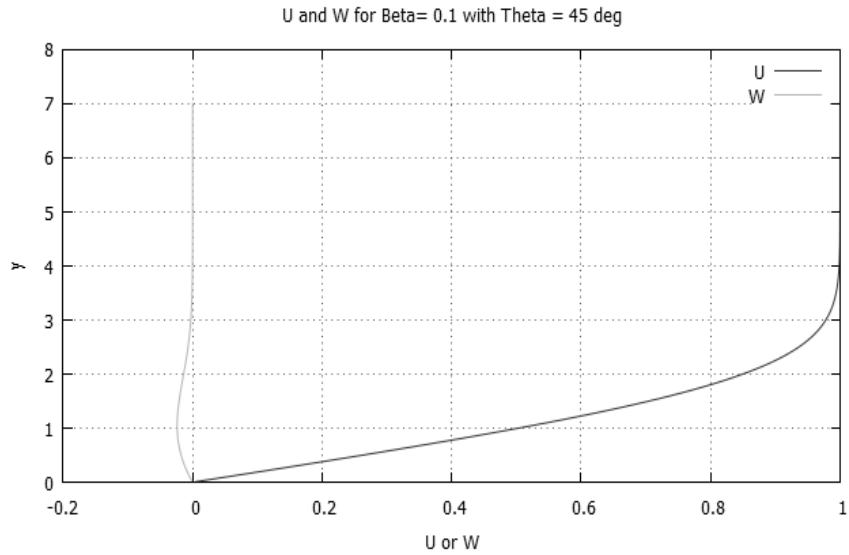


Figure 8. Velocity profiles for $\beta_H = 0.1$ and $\theta = 45^\circ$ [16].

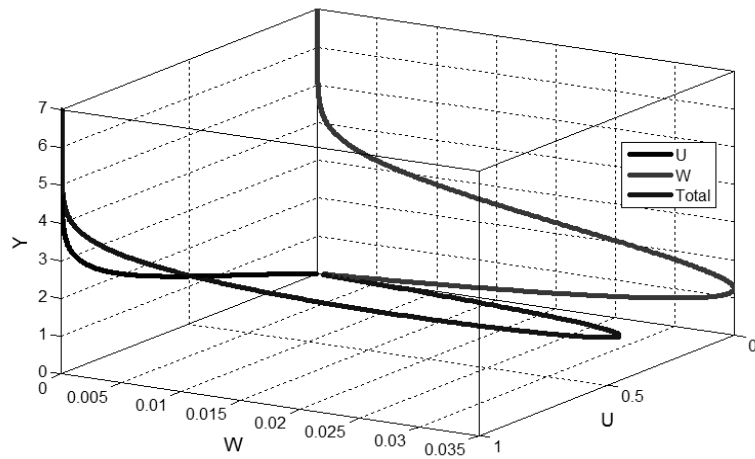


Figure 9. Composite profile corresponding to $\beta_H = -0.1$ and $\theta = 45^\circ$ [16].

Figure 10 depicts the neutral stability curves for various flow angles and $\beta_H = -0.1$ (adverse pressure gradient). As can be seen, as the flow angle increases, the unstable regions gets smaller and the critical Reynolds number increases, i.e. flow is stabilized.

Figure 11 illustrates the neutral stability curves for a favourable pressure gradient flow, $\beta_H = 0.1$. In this case the trend is the opposite of Figure 10, i.e. the flow is destabilized with increasing flow angle.

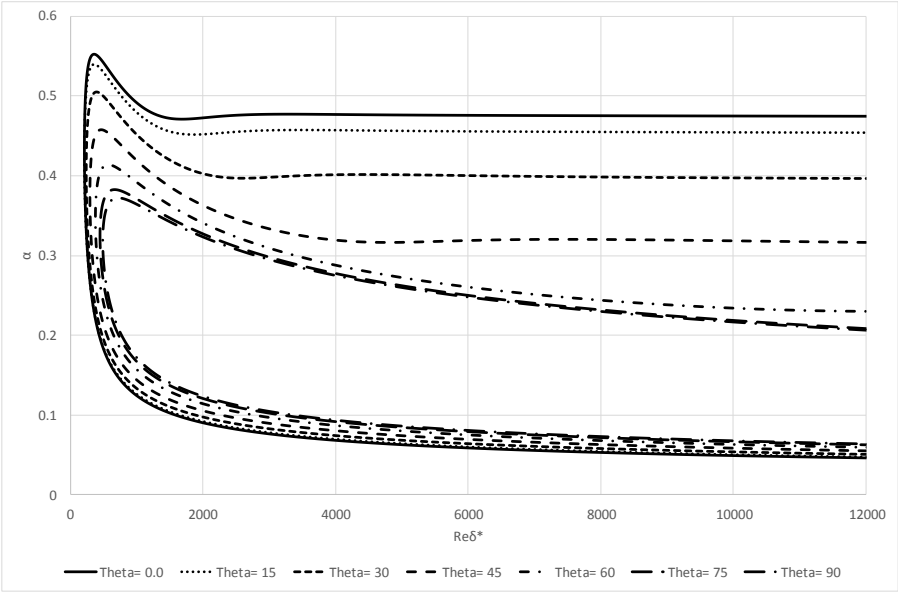


Figure 10. Neutral stability curves for different flow angles for $\beta_H = -0.1$ [16].

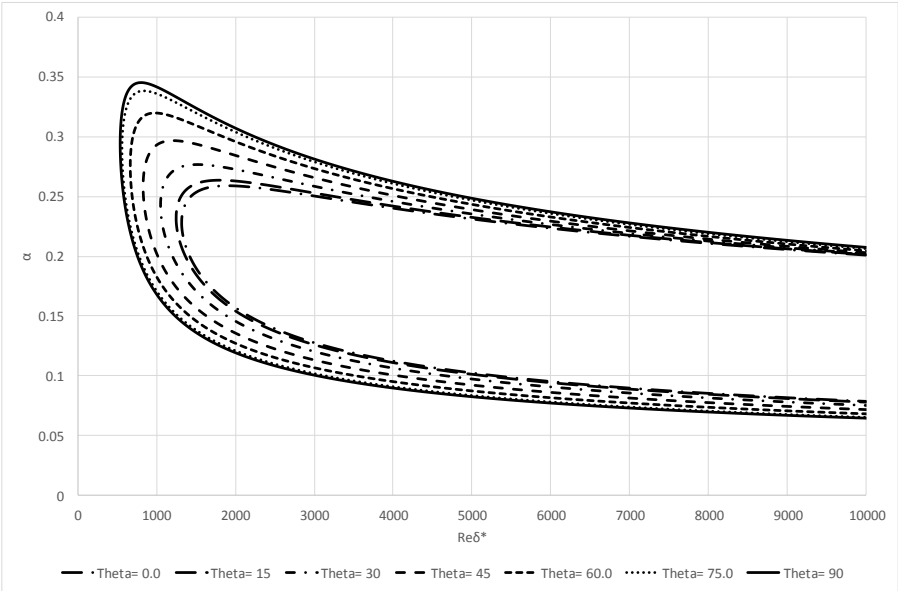


Figure 11. Neutral stability curves for different flow angles for $\beta_H = 0.1$ [16].

Finally, Figure 12 summarizes the analysis mentioned above by presenting the variation of the critical Reynolds number as a function of the flow angle for three different values of the Hartree parameter. The three most important inferences are as follows:

- As the flow angle increases, the critical Reynolds numbers decreases for a flow with favourable pressure gradient $\beta_H = 0.1$, i.e. the flow is destabilized.
- As the flow angle increases, the critical Reynolds numbers increases for a flow with adverse pressure gradient $\beta_H = -0.1$, i.e. the flow is stabilized.
- The flow angle has no effect on the stability of a Blasius flow, $\beta_H = 0$.

As a result, the most important conclusion of the analysis is that the flow angle decreases the effect of the pressure gradient.

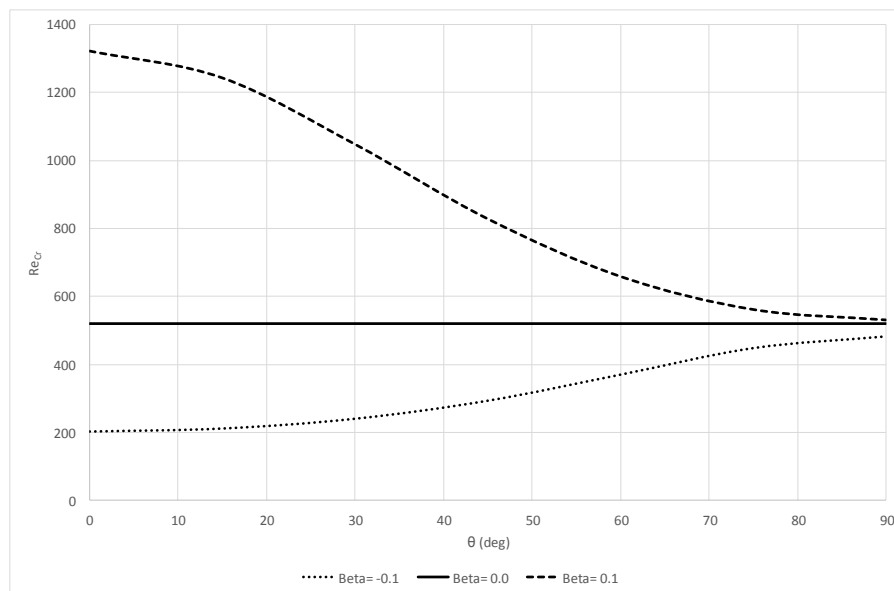


Figure 12. Effect of flow angle on the critical Reynolds number for $\beta_H = -0.1, 0, 0.1$ [16].

4. Conclusions

Linear Stability Theory is outlined and the stability equations are derived using text-book approaches. Main aspects of the theory, including method of small disturbances, method of normal modes, temporal and spatial formulations, Gaster's Transformation, Orr-Sommerfeld equation and Squire's Theorem are explained. Solution of the stability problem for the temporal amplification formulation is explained and two illustrative cases are studied, namely two- and three-dimensional boundary layer flows. The test cases emphasize the effect of two very important parameters on the stability of flows, namely the pressure gradient and crossflow. The approach chosen in the manuscript is hoped to familiarize the reader with basic concepts and to make understanding and following the related literature easier.

References

- [1] White, F. M., *Viscous Fluid Flow, Third Ed.*, McGraw-Hill, 2006.
- [2] Schlichting, H., *Boundary-Layer Theory, Seventh Ed.*, McGraw-Hill, 1979.
- [3] Lord Rayleigh, On the stability of certain fluid motions, *Proc. Math. Soc. London* 19, 1887.
- [4] Prandtl, L., Bemerkungen über die Entstehung der Turbulenz, *ZAMM I*, 1921.
- [5] Tollmien, W., Über die Entstehung der Turbulenz, Engl. Transl. in NACA TM 609, 1931.
- [6] Schlichting, H., Zur Entstehung der Turbulenz bei der Plattenströmung, *ZAMM 13*, 1933.
- [7] Schubauer, G. B. and Skramstad, H. K., Laminar boundary-layer oscillations and stability of laminar flow, National Bureau of Standards Research paper 1772, 1947.
- [8] Van Dyke, M., *an Album of Fluid Motion*, Parabolic Press, 1982.
- [9] Pinna, F., Stability of boundary-layer flows in different regimes, in *Progress in Flow Instability Analysis and Laminar-Turbulent Transition Modelling*, Von Karman Institute for Fluid Dynamics Lecture Series, 2014.
- [10] Gaster, M., A note on the relation between temporally-increasing and spatially-increasing disturbances in hydrodynamic stability, *J. Fluid Mech.* 14, 1962.
- [11] Özgen, S., Two-Layer Flow Stability in Newtonian and Non-Newtonian Fluids, Ph.D. Thesis, Von Karman Institute for Fluid Dynamics and Université Libre de Bruxelles, 1999.
- [12] Mack, L. M., Boundary-layer linear stability theory, in *Special Course on Stability and Transition of Laminar Flow*, AGARD Report 709, 1984.
- [13] Özgen, S., Atalayer Kırçalı, S., Linear stability analysis in compressible, flat-plate boundary-layers, *Theor. Comput. Fluid Dyn.* 22, 2008.
- [14] Özgen, S., Effect of heat transfer on stability and transition characteristics of boundary-layers, *Int. J. Heat Mass Transfer* 47, 2004.
- [15] Özgen, S., Dursunkaya, Z., Ebrinç, A. A., Heat transfer effects on the stability of low speed plane Couette-Poiseuille flow, *Heat Mass Transfer* 43, 2007.
- [16] Yang, Y., Özgen, S., Investigation of the stability characteristics of three-dimensional flows using the Linear Stability Theory (in Turkish), in *V. National Aerospace Conference*, Kayseri, Turkey, 2014.